MOLECULAR AND CELLULAR BIOLOGY, July 2005, p. 5712–5724 Vol. 25, No. 13
0270-7306/05/$08.00+0 doi:10.1128/MCB.25.13.5712–5724.2005

Coactivator Recruitment Is Essential for Liganded Thyroid Hormone Receptor To Initiate Amphibian Metamorphosis

Bindu Diana Paul, Liezhen Fu, Daniel R. Buchholz, and Yun-Bo Shi*

Laboratory of Gene Regulation and Development, National Institute of Child Health and Human Development, National Institutes of Health, Bldg. 18T, Rm. 106, Bethesda, Maryland 20892

Received 14 September 2004/Returned for modification 19 October 2004/Accepted 25 March 2005

Thyroid hormone receptors (TRs) can repress or activate target genes depending on the absence or presence of thyroid hormone (T3), respectively. This hormone-dependent gene regulation is mediated by recruitment of corepressors in the absence of T3 and coactivators in its presence. Many TR-interacting coactivators have been characterized in vitro. In comparison, few studies have addressed the developmental roles of these cofactors in vivo. We have investigated the role of coactivators in transcriptional activation by TR during postembryonic tissue remodeling by using amphibian metamorphosis as a model system. We have previously shown that steroid receptor coactivator 3 (SRC3) is expressed and upregulated during metamorphosis, suggesting a role in gene regulation by liganded TR. Here, we have generated transgenic tadpoles expressing a dominant negative form of SRC3 (F-dnSRC3). The transgenic tadpoles exhibited normal growth and development throughout embryogenesis and premetamorphic stages. However, transgenic expression of F-dnSRC3 inhibits essentially all aspects of T3-induced metamorphosis, as well as natural metamorphosis, leading to delayed or arrested metamorphosis or the formation of tailed frogs. Molecular analysis revealed that F-dnSRC3 functioned by blocking the recruitment of endogenous coactivators to T3 target genes without affecting corepressor release, thereby preventing the T3-dependent gene regulation program responsible for tissue transformations during metamorphosis. Our studies thus demonstrate that coactivator recruitment, aside from corepressor release, is required for T3 function in development and further provide the first example where a specific coactivator-dependent gene regulation pathway by a nuclear receptor has been shown to underlie specific developmental events.

Thyroid hormone receptors (TRs) are believed to mediate most, if not all, of the vast, diverse biological effects of thyroid hormone (T3) (38, 56, 62, 75). TRs belong to the superfamily of nuclear hormone receptors, which also includes steroid hormone receptors and 9-*cis* retinoic acid receptors (RXRs), and function in vivo most likely as heterodimers with RXRs (38, 41, 66, 75). TR/RXR heterodimers bind to T3 response elements (TREs) constitutively and repress or activate gene expression in a T3-dependent manner by recruiting corepressors or coactivators, respectively.

In vitro and cell culture studies have led to the isolation and characterization of many TR-interacting cofactor complexes (31, 34, 48, 75, 79). Among them, the best-studied corepressor complexes are those containing the nuclear receptor corepressor N-CoR (27) and the silencing mediator of retinoid and thyroid hormone receptor SMRT (7). Both N-CoR and SMRT exist in multiple histone deacetylase (HDAC)-containing complexes (23, 34, 40, 79). Recent studies suggest that TR most likely utilizes the complexes that contain HDAC3 and TBL1 (for transducin beta-like protein 1) or TBLR1 (for TBL1-related protein) (23, 28, 40, 63, 64, 76, 78).

Among the coactivators that interact with TR directly, the steroid receptor coactivator (SRC) family, which comprises three members (SRC1/NCoA-1, SRC2/TIF2/GRIP1, and SRC3/pCIP/ACTR/AIB-1/RAC-3/TRAM-1) has been the focus of intense studies (6, 26, 39, 45, 61, 68). The SRC proteins bind TR and other nuclear receptors in a ligand-dependent manner through LXXLL (L, leucine; X, any amino acid) motifs, which are indispensable for the interaction (11, 24, 45, 67, 68). The LXXLL motifs form short amphipathic α-helices, with the leucine residues forming a hydrophobic surface on one face of the helix (44, 59, 65). These motifs bind a hydrophobic cleft in the ligand-binding domain of liganded nuclear receptors (13). Three such LXXLL motifs are localized in the central region of these proteins and form the receptor interaction domain (RID). SRC proteins function as bridging factors to recruit chromatin-modifying enzymes, including methylases and histone acetyltransferases.

It remains to be determined how TR utilizes these coactivators in vivo, especially during development when TR regulates different genes in different cell types. This lack of information on the in vivo function of the coactivators in developmental gene regulation by TR is attributed largely to the difficulty in studying TR function in the uterus-enclosed mammalian embryos, despite the fact that T3 deficiency has long been known to cause severe developmental defects, including cretinism (25). The effects of T3 on development take place mainly during perinatal period, when T3 levels in the plasma are high (4, 25, 37).

It is unclear whether and how TR mediates the developmental effects of T3 because of the existence of nongenomic mechanisms through cytosolic T3-binding proteins (10). Studies with TR knockout mice have provided some in vivo evidence to support a critical role of TRs in mediating T3 signal in development. Interestingly, mice lacking TRα or TRβ or both have much less severe developmental defects than those lacking T3 (15–17, 20, 22, 70). Furthermore, transgenic mice harboring a dominant negative form of the corepressor N-CoR containing

* Corresponding author. Mailing address: NIH, LGRD, NICHD, Building 18T, Rm. 106, Bethesda, MD 20892. Phone: (301) 402-1004. Fax: (301) 402-1323. E-mail: shi@helix.nih.gov.

only the receptor-interacting domain in the liver exhibit upregulated T3-inducible genes (14). Finally, many studies with tissue culture cells and frog oocytes show that the bulk of the increases in target gene expression by T3 appears to be due to the release of repression caused by unliganded TR. These studies thus leave unresolved the possibility that corepressor release, not coactivator recruitment, may be the major effect of T3 on gene regulation during development.

Here, we use amphibian metamorphosis as a model to study the role of coactivators in T3 function during development. Amphibian metamorphosis is a T3-dependent process that bears strong similarities to postembryonic development in mammals (56, 62). Unlike mammalian development, amphibian metamorphosis can be easily manipulated by blocking the synthesis of endogenous T3 or by adding physiological concentrations of T3 to the tadpole rearing water, even though different organs and/or tissues undergo vastly different transformations (12, 56).

Using this model system, we have shown previously that the mRNAs of TR interacting cofactors SRC2, SRC3, and p300 are expressed during metamorphosis, among which SRC3 is upregulated during both natural and T3-induced metamorphosis, supporting a role for this coactivator (47). To directly investigate the role of coactivator recruitment by TR in mediating the developmental effects of T3 in vivo, we introduced a dominant negative form of SRC3 (F-dnSRC3) into developing animals through sperm-mediated transgenesis. We showed that F-dnSRC3 inhibits both natural and T3-induced metamorphosis and the expression of TR target genes by specifically blocking coactivator recruitment but not corepressor release. These results thus identify an essential role of coactivator binding to TR beyond corepressor release in postembryonic development.

MATERIALS AND METHODS

Cloning and constructs. The dominant negative SRC3, F-dnSRC3, was generated by PCR amplification of the sequences encompassing the receptor interaction domain of *Xenopus laevis* SRC3 (amino acids [aa] 600 to 751) (35). The construct was generated to encode a fusion protein with an N-terminal Flag epitope tag (8), followed by the simian virus 40 (SV40) nuclear localization signal (NLS) (5) using a 5′ primer containing the sequences encoding these fusion peptides in frame with the SRC3 coding sequence. The primers used were (5′ to 3′) AGATCTACCGGTGCCATGGACTACAAAGACGATGACGATAAAG GATCC**CCAAAGAAGAAGAAGCGTAAGGTACTCGAG**ATGATATTTGAAG GGTCGGAGA (the Flag tag is underlined and the NLS is shown in boldface type) and CTAGTCACTAGTGAATTCTCACTTGGCCAGTGGGTCCTTCC AGTC. For expression and detection in frog oocytes, the PCR product was cloned into the T7Ts expression vector (a gift from G. J. C. Veenstra, University of Nijmegen), which is based on the pGEM-4Z vector (Promega) and contains the 5′ and 3′-untranslated regions of the *X. laevis* β-globin gene flanking the multiple cloning sites.

For transgenesis, F-dnSRC3 was subcloned into the vector pCGCG (18) under the control of the cytomegalovirus (CMV) promoter, replacing the original green fluorescent protein (GFP) fragment at this location and resulting in the double-promoter construct pCF-dnSRC3CG, which also has the gene for GFP driven by the eye lens-specific γ-*crystallin* promoter.

Animals, transgenesis, and animal treatment. Wild-type tadpoles of the African clawed frog *Xenopus laevis* were obtained from Xenopus I, Inc. (Dexter, MI), and developmental stages were determined according to Nieuwkoop and Faber (43). Adult female frogs used for oocyte preparation were obtained from NASCO (Fort Atkinson, WI).

Transgenesis was carried out using *X. laevis* as described previously (18) using the double-promoter construct pCF-dnSRC3CG. Transgenic animals were identified by GFP expression in the eye lens due to the presence of the second promoter, the γ-*crystallin* promoter, driving the expression of GFP.

To study the effect of transgene on T3-induced tail resorption and other external changes, 1-week-old transgenic tadpoles were treated for 7 days with 10 nM T3 diluted in 0.1× MMR (10 mM NaCl–0.2 mM KCl–0.1 mM $MgCl_2$–0.2 mM $CaCl_2$–0.5 mM HEPES, pH 7.5). Both wild-type and transgenic animals were treated in the same container to ensure similar conditions of treatment. To study the effect of the transgene on limb development and changes in the intestine, stage 54 animals were treated with the indicated amount of T3 (two animals per liter of deionized, dechlorinated water). These tadpoles were sacrificed by decapitation after anesthesia (cooling on ice) to isolate tissues for molecular analyses.

Oocyte injection and immunoprecipitation. pSP64-TR, pSP64-RXR (71), and T7Ts-Flag-dnSRC3 were used to synthesize the corresponding mRNAs in vitro with a T7 or SP6 in vitro transcription kit (mMESSAGE mMACHINE; Ambion). The mRNA, at a concentration of 5.75 ng/oocyte, was microinjected into the cytoplasm of 20 *X. laevis* stage VI oocytes. After incubation overnight at 18°C, the oocytes were lysed by being pipetted in lysis buffer (20 mM HEPES, pH 7.5, 5 mM KCl, 1.5 mM $MgCl_2$, 1 mM EGTA, 10 mM glycerophosphate, 150 mM NaCl, 0.1% NP-40, 1 mM dithiothreitol, 0.2 mM phenylmethylsulfonyl fluoride, and protease inhibitor mixture [Roche Applied Science]). After centrifugation at 14,000 rpm for 10 min at 4°C, the supernatant was used for immunoprecipitation with anti-Flag-M2-agarose beads (Sigma). Each lysate was incubated with the beads for 4 h and washed three times in the lysis buffer. The immunoprecipitates were boiled in sodium dodecyl sulfate (SDS) loading buffer, separated on an SDS-polyacrylamide gel, and immunoblotted with indicated antibodies.

Luciferase assays. The cytoplasm of groups of stage VI oocytes was injected with mRNAs encoding TR, RXR, and/or F-dnSRC3 (5.75 ng per oocyte). The reporter plasmid DNA (0.33 ng/oocyte), which contained the T3-dependent *TRβA* promoter driving the expression of the firefly luciferase (1) was injected into the oocyte nucleus, together with a control construct which contained the herpes simplex virus *tk* promoter driving the expression of *Renilla* luciferase (0.03 ng/oocyte). Following incubation overnight at 18°C in the absence or presence of 100 nM T3, oocytes were prepared for luciferase assay by the Dual-Luciferase Reporter Assay system (Promega), according to the manufacturer's recommendations.

Protein extraction and Western blot analysis. Isolated tissues from wild-type and transgenic tadpoles at stage 54 were homogenized on ice in lysis buffer [10 mM Tris-HCl, pH 7.5, 150 mM NaCl, 5 mM EDTA, 1% Triton X-100, 200 M 4-(2-aminoethyl)-benzenesulfonylfluoride HCl, 5 μg/ml aprotinin, 2 μg/ml leupeptin, and 1 μg/ml pepstatin]. The homogenate was kept on ice for 30 min before centrifugation for 15 min at 4°C (11,000 × *g*). Equal amounts of the protein extract were then analyzed by Western blotting with anti-Flag antibodies to detect the expression of the transgene.

Chromatin immunoprecipitation (ChIP) assays. The ChIP assay with *Xenopus* oocytes was performed as described previously (63). For the ChIP assay with tadpole tissues, four tadpoles per treatment group were used. Wild-type and transgenic tadpoles were treated with 10 nM T3 for 2 days in the same container. The ChIP assay was performed as described previously (9, 54) with minor modifications (64). The following antibodies were used in the assay: anti-*Xenopus* TR (71), anti-acetylated histone H4 (Upstate Biotechnology, Lake Placid, N.Y.), anti-Flag M2-agarose (Sigma), anti-*Xenopus* SRC3 (generated in rabbits by coinjecting the peptides SGEKRRREQESK and DHLEDGSNLDARQRYE), and anti-*Xenopus* SMRT antibody (generated by immunizing a rabbit with the polypeptide KSKKQEMIKKLSTTNRSEQE, located in a 2-kb cDNA fragment corresponding to the C-terminal part encompassing the TR-binding domain of the *Xenopus laevis* SMRT) (64). The primers used in the oocyte ChIP assay were (5′ to 3′ direction) TGCCTGTGTCTATACTGATGGGAT and CATTTTACCAA CAGTACCGGAATGC, producing a 190-bp fragment containing the TRE region of the construct TRE-Luc.

The DNA from the ChIP assay with tadpole tissues was analyzed by quantitative PCR in duplicate on an ABI 7000 (Applied Biosystems) system using promoter-specific primers and 6-carboxyfluorescein-labeled *Taq*Man probes (Applied Biosystems). To ensure the validity of the PCR for each assay, six twofold serial dilutions from a large batch of ChIP input DNA prepared from intestines prepared especially to serve as standards were used for the quantification of the experimental samples. The calculated standard curves ranged in slope from −3.30 to −3.50, where theoretical amplification has a slope of −3.32. Also included was a no-template control, where double-distilled water was added instead of sample DNA as a control for PCR product contamination. Results from the experimental samples were within the range of the standard curve. The primers used for the quantitative PCR were as follows (5′ to 3′): CCCCTATC CTTGTTCGTCCTC and GCGCTGGGCTGTCCT for the TRE region of the *TRβA* promoter and GGACGCACTAGGGTTAAGTAAGG and TCTCCCAA CCCTACAGAGTTCAA for the TRE region of the *TH/bZIP* promoter. The 6-carboxyfluorescein-labeled probes were (5′ to 3′) CCTAGGCAGGTCATTTC

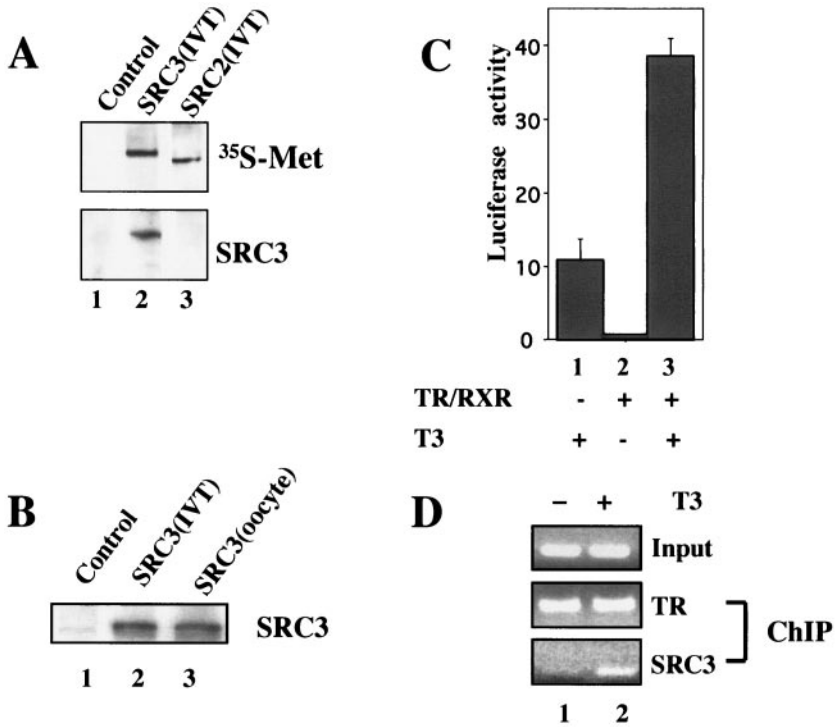

FIG. 1. The *Xenopus laevis* SRC3 protein is recruited by TR to target genes in the frog oocyte. (A) The anti-SRC3 antibody specifically recognizes the *Xenopus laevis* SRC3 protein. The two SRC family proteins cloned from *Xenopus laevis*, SRC3 and SRC2 (lanes 2 and 3), were translated in vitro in the presence of ^{35}S-Met and analyzed on an 8 to 16% Tris glycine SDS gel. The proteins were transferred to a membrane and blotted with polyclonal anti-SRC3 antibodies. Top, ^{35}S-Met signal; bottom, Western blot signal. Lane 1, control (unprogrammed rabbit reticulocyte lysate). (B) The anti-SRC3 antibody recognizes endogenous SRC3 protein in *Xenopus* oocyte nuclei. Lanes 1 and 2, unprogrammed rabbit reticulocyte lysate and in vitro-translated SRC3, respectively; lane 3, protein extract from isolated nuclei (germinal vesicles) of *Xenopus* oocytes. (C) Transcription from the T3-inducible promoter of the *Xenopus TR*β*A* gene is regulated by TR/RXR in a ligand-dependent manner. The cytoplasm of oocytes was injected with mRNAs for TR (5.75 ng/oocyte) and RXR (5.75 ng/oocyte). The firefly luciferase reporter construct TRE-Luc (0.33 ng/oocyte) was then injected into the nucleus together with the control *Renilla* luciferase plasmid (0.03 ng/oocyte), followed by incubation overnight at 18°C with or without 100 nM T3. The oocytes were harvested and lysed, and the ratio of firefly luciferase from TRE-Luc to that from the control *Renilla* luciferase plasmid was determined for each oocyte. The average and standard deviations from four measurements are plotted. (D) SRC3 is recruited to the TRE in a ligand-dependent manner. Groups of oocytes were injected with mRNAs for TR and RXR and treated as described above. ChIP assays were carried out using antibodies against TR and SRC3 to detect the occupancy of TR and SRC3 on the promoter. The presence of TRE in the immunoprecipitated samples was detected by PCR using primers flanking the TRE. The products were analyzed on a 2% agarose gel and visualized by ethidium bromide staining. The DNA prior to immunoprecipitation was amplified by PCR as an input control.

and ATGAGGCTGAGCATTCA for the *TR*β*A* and the *TH/bZIP* promoters, respectively.

RNA isolation and reverse transcriptase PCR (RT-PCR). RNA was isolated using the Trizol reagent (Invitrogen) per the manufacturer's recommendations. RT-PCRs were carried out with the Superscript One-Step RT-PCR kit (Invitrogen). The expression of the ribosomal protein L8 (Rpl8) was used as an internal control (58). The sequences of the primers used were (5′ to 3′) CGTGGTGCT CCTCTTGCCAAG and GACGACCAGTACGACGAGCAG for *rpl8* (58), CC TGATGCATGCAAAACT and GTTCATCCTGGAAAGCAG for *ST3* (46), CACTTAGCAACAGGGATCAGC and CTTGTCCCAGTAGCAATCATC for *TH/bZIP* (19), ATAGTTAATGCGCCCGAGGGTGGA and CTTTTCT ATTCTCTCCACGCTAGC for *TR*βA (74), CATCATGATTCCTGGTAA CCGA and AAATTTCCATTTTCTGCTGTGC for *BMP-4* (42), and GGGC AGTGGACATCACCAC and GTTGACCTTGGTCTGGGCC for *xhh* (60). The sequences of the primers used for the detection of F-dnSRC3 in transgenic animals were (5′ to 3′) ACCGGTGCCATGGACTAC and CTAGT CACTAGTGAATTCTCACTTGGCCAGTGTCCTTCCAGTC. A total of 0.5 μg of total RNA was used in a 25-μl reaction mixture, under the following reaction conditions: 42°C for 30 min for the RT reaction, followed by 21 to 25 cycles, each consisting of 94°C for 30 s, 55°C for 30 s, and 72°C for 30 s. The resulting products were analyzed on an agarose gel stained with ethidium bromide.

Histological analysis of the intestine. The intestines of the tadpoles were dissected and fixed for 2 h at room temperature in 4% paraformaldehyde–60% phosphate-buffered saline, cryoprotected in 0.5 M sucrose in 60% phosphate-buffered saline and embedded in OCT medium (TissueTek). The intestines were sectioned in a cryotome at 7.5 μm. Sections were visualized with methyl green pyronin Y (Muto, Tokyo, Japan) (29).

RESULTS

TR recruits SRC3 during transcriptional activation in *Xenopus laevis* oocytes. Our previous expression studies have shown that both SRC2 and SRC3 are expressed and that SRC3 is upregulated during both natural and T3-induced metamorphosis. We were thus interested in investigating the roles of such TR-binding coactivators in this postembryonic process by altering coactivator recruitment by TR through transgenesis. For this purpose, we reasoned that this might be accomplished by introducing a dominant negative form of SRC3 to inhibit the binding of endogenous coactivators to liganded TR. As a first step, we generated polyclonal antibodies against peptides derived from *Xenopus laevis* SRC3. The specificity of the antibody was verified by Western blotting using in vitro-translated *Xenopus* SRC3 and SRC2 (Fig. 1A), the two SRC proteins cloned so far from *Xenopus laevis*. In addition, the

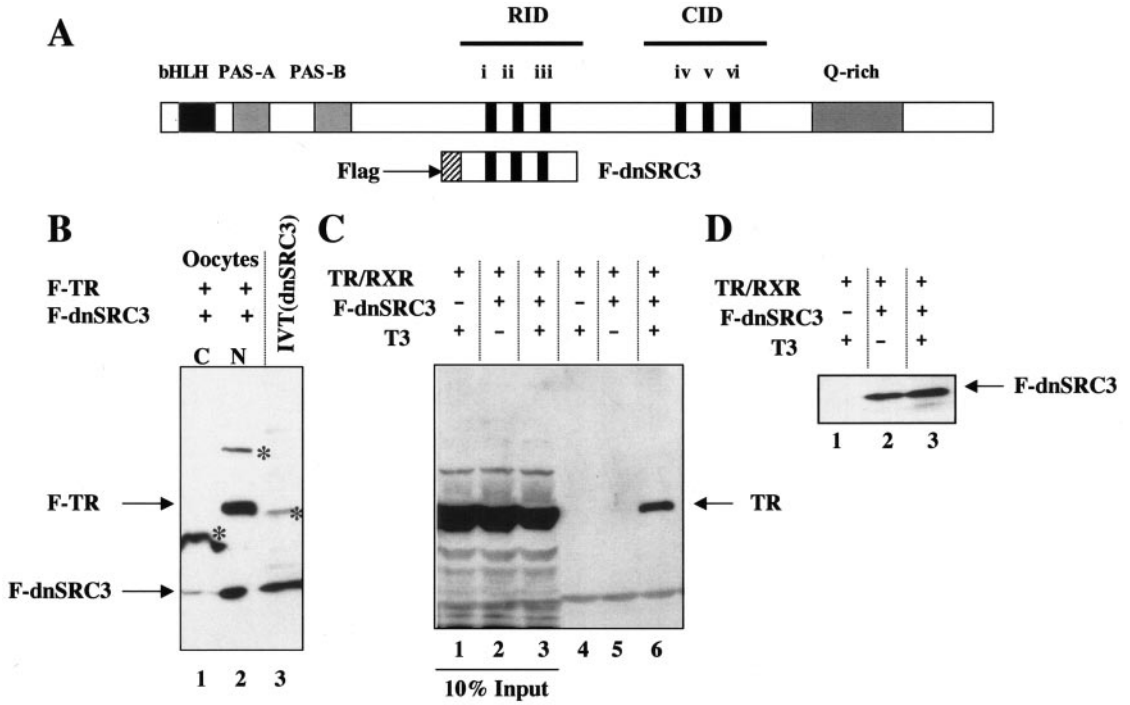

FIG. 2. Generation and characterization of a dominant negative SRC3 (F-dnSRC3). (A) Schematic representation of the full-length SRC3 illustrating the organization of various domains: bHLH/PAS (basic helix-loop-helix and PAS dimerization domains) RID, and CID (CBP/p300 interaction domain). The LXXLL motifs present in the protein are numbered from i to vi. A glutamine-rich (Q-rich) region is present towards the C-terminal end of the protein. The dominant negative form, dnSRC3 (aa 600 to 751), which comprises the LXXLL motifs i to iii, forming the RID, and fused to an N-terminal peptide containing the Flag tag and nuclear localization sequences, is shown below. (B) The F-dnSRC3 protein is localized in the nucleus. Oocytes were injected with mRNAs (5.75 ng/oocyte) for F-TR, RXR, and F-dnSRC3 and incubated overnight. The oocytes were then harvested, and nuclei were dissected manually under a light microscope. The nuclei and cytoplasmic components were resuspended in 1× SDS lysis buffer, boiled for 5 min, resolved on an 8 to 16% Tris glycine-SDS gel, and visualized by Western blotting using anti-Flag antibody. Lane 1, C, the cytoplasmic extracts of *Xenopus* oocytes overexpressing F-dnSRC3 and F-TR; lane 2, N, the corresponding nuclear extracts; lane 3, IVT, in vitro-translated F-dnSRC3. The asterisks indicate cross-reacting bands recognized by the antibody. (C) F-dnSRC3 interacts with TR/RXR in a T3-dependent manner. Groups of oocytes were injected with 5.75 ng of TR, RXR, and F-dnSRC3 mRNAs and incubated overnight in the presence or absence of 100 nM T3. Twenty *Xenopus* oocytes were used for each immunoprecipitation with anti-Flag M2 antibody conjugated to Sepharose beads, followed by Western blot analysis using anti-TR antibody. Lanes 1 to 3, 10% input samples; lanes 4 to 6, immunoprecipitation with anti-Flag antibody. (D) Western blotting of input samples shown in panel C with anti-Flag antibody shows similar expression of F-dnSRC3 in the injected oocytes.

antibody was raised against peptides from SRC3 that did not exhibit sequence similarity to any region of SRC1 cloned so far from other species (not shown), making it unlikely to recognize endogenous *Xenopus laevis* SRC1.

To study the involvement of SRC3 in T3-mediated transcriptional activation, we utilized the frog oocyte system, which allows the analysis of gene activation by TR in the context of chromatin (71). First, we showed that endogenous SRC3 was present in the nuclei of *Xenopus* oocytes (Fig. 1B, lane 3). Next, a reporter construct, TRE-Luc, which harbors the T3-dependent *Xenopus TRβA* promoter fused to the firefly luciferase gene (1), was microinjected into the nuclei of *Xenopus* oocytes together with a plasmid harboring the *Renilla* luciferase gene as an internal control. The mRNAs encoding TR and RXR were microinjected subsequently into the cytoplasm of the oocytes. Following an overnight incubation in the presence or absence of 100 nM T3, oocytes were harvested and assayed for luciferase activity. As expected, in the absence of T3, basal activity from TRE-Luc was repressed by TR and RXR (71), while in the presence of T3, the promoter was activated (Fig. 1C). Finally, to determine whether SRC3 was involved in this gene activation by TR, we carried out ChIP assays using antibodies against TR and SRC3. The results revealed that while TR binds to the TRE region constitutively, endogenous SRC3 was recruited to the *TRβA* promoter only in the presence of T3 (Fig. 1D), suggesting that liganded TR recruits SRC3 to activate the promoter in vivo.

A dominant negative SRC3 inhibits gene activation by TR in the frog oocyte. To generate a dominant negative form of SRC3, we reasoned that a truncated protein comprising only the receptor interaction domain of SRC3 might be able to function as a dominant negative inhibitor of coactivator binding to TR, thus inhibiting gene activation by liganded TR. Therefore, we generated a truncated form of SRC3 (Fig. 2A), F-dnSRC3, consisting of an N-terminal Flag tag, followed by the SV40 NLS and the receptor interaction domain of SRC3 (aa 600 to 751) (35). To verify the expression and localization of F-dnSRC3, its mRNA was synthesized in vitro and microinjected into the oocyte cytoplasm. As a control, the mRNA encoding Flag-tagged *Xenopus* TR (F-TR), which localizes to the nucleus, was coinjected. After overnight incubation, the nuclear and cytoplasmic fractions of the injected oocytes were

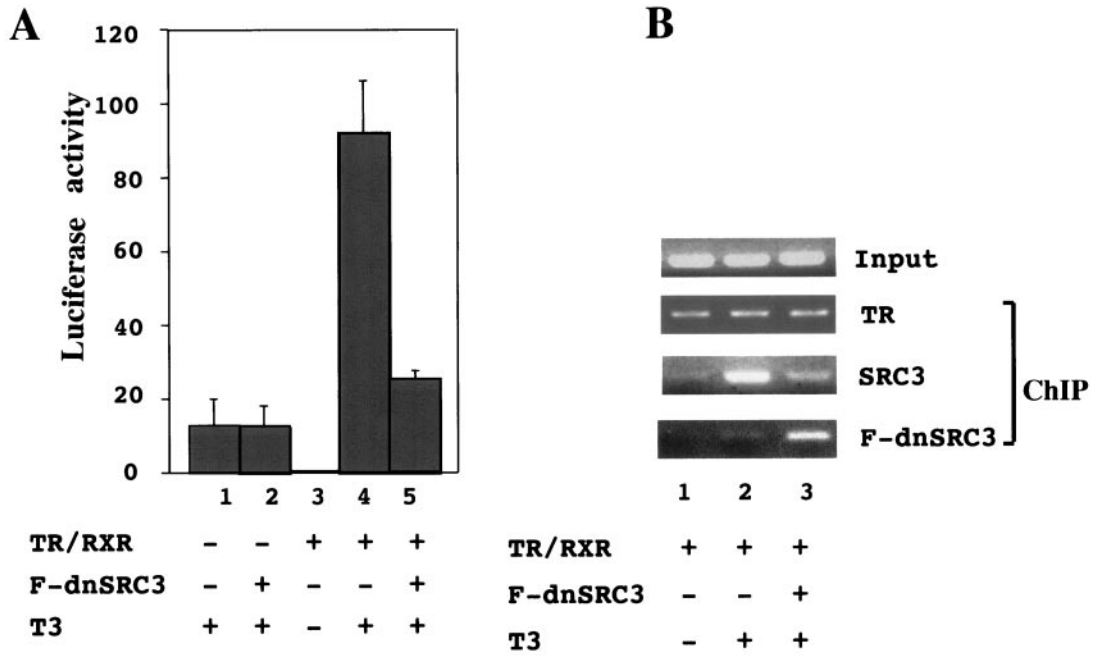

FIG. 3. (A) F-dnSRC3 inhibits T3-induced transcription from the *TRβA* promoter. The mRNAs for TR, RXR, and F-dnSRC3 (5.75 ng/oocyte) were injected into the cytoplasm of oocytes. The firefly luciferase reporter vector (0.33 ng/oocyte) (TRE-Luc) was then injected into the nucleus together with the control *Renilla* luciferase plasmid (0.03 ng/oocyte). After overnight incubation at 18°C with or without 100 nM T3, oocytes were harvested and assayed for transcription from TRE-Luc. The ratio of firefly luciferase activity from TRE-Luc to that from the control *Renilla* luciferase plasmid was determined for each oocyte, and the average from six oocytes was plotted together with the standard deviation. Note that as expected, unliganded TR/RXR repressed basal activity of the target promoter; the addition of T3 released the repression and further activated the promoter. F-dnSRC3 inhibited T3 activation but not basal activity. (B) F-dnSRC3 competes against endogenous SRC3 for recruitment to the *TRβA* promoter in a ligand-dependent manner. A total of 5.75 ng of TR, RXR, or F-dnSRC3 mRNAs was injected into the cytoplasm of each *Xenopus* oocyte. The construct TRE-Luc was injected into the nucleus. The oocytes were treated with or without 100 nM T3 as indicated. After overnight incubation, ChIP analysis was carried out using anti-TR, anti-SRC3, or anti-FLAG antibodies.

isolated and subjected to Western blotting using the anti-Flag antibody. The results showed that both F-TR and F-dnSRC3 were efficiently expressed and localized in the nucleus (Fig. 2B).

To investigate the ability of F-dnSRC3 to interact with the TR/RXR heterodimer, we then carried out coimmunoprecipitation assays. The mRNAs encoding *Xenopus* TR, RXR, and F-dnSRC3 were injected into the cytoplasm of oocytes. After incubation overnight in the absence or presence of 100 nM T3, extracts prepared from groups of oocytes were incubated with the anti-Flag antibody. Immunoprecipitated samples were then probed with anti-TR antibodies, which revealed that F-dnSRC3 protein interacted with TR in a ligand-dependent manner (Fig. 2C, lanes 5 and 6). Control Western blotting of the extracts before immunoprecipitation with anti-Flag antibody showed that similar amounts of F-dnSRC3 were present in oocytes incubated in the absence or presence of T3 (Fig. 2D, lanes 2 and 3).

We next tested the ability of F-dnSRC3 to inhibit transcriptional activation by liganded TR. Again, we microinjected the reporter vector harboring the T3-dependent *Xenopus TRβA* promoter into the nuclei of oocytes together with the internal control plasmid harboring the *Renilla* luciferase gene. The cytoplasm of groups of oocytes was injected with mRNAs encoding TR, RXR, and/or F-dnSRC3. The oocytes were incubated overnight in the absence or presence of T3, followed by luciferase assays. As shown in Fig. 3A, F-dnSRC3 had no effect on basal transcription in the absence of TR/RXR (Fig. 3A, lanes 1 and 2). However, the activation by TR/RXR in the presence of T3 was inhibited by F-dnSRC3 (Fig. 3A, compare lanes 5 and 4). To investigate whether this dominant negative effect of F-dnSRC3 was due to its T3-dependent recruitment to the promoter, ChIP assays were carried out using antibodies against TR and F-dnSRC3. The results revealed that F-dnSRC3 was recruited to the promoter in a T3-dependent fashion, whereas TR bound constitutively to the *TRβA* promoter in the oocyte (Fig. 3B). Moreover, in the presence of F-dnSRC3, the T3-dependent recruitment of endogenous SRC3 to the promoter was impaired (Fig. 3B). These results suggest that F-dnSRC3 functions as an effective dominant negative to block endogenous coactivators in gene regulation by TR and that the recruitment of SRC3 or other TR-binding coactivators by liganded TR is essential for gene activation in vivo.

Transgenic overexpression of F-dnSRC3 inhibits T3-induced metamorphosis. To investigate whether F-dnSRC3 may affect gene regulation by TR and metamorphosis in vivo, we introduced it into developing animals through transgenesis using the restriction enzyme-mediated integration method (36). The expression of F-dnSRC3 in transgenic animals was driven by the constitutively active CMV promoter. We used a double-promoter construct that also harbored GFP under the control of the γ-*crystallin* promoter (Fig. 4A) (18), which is functional only in the eye lens. This allowed us to rear both wild-type and transgenic animals together to avoid variations in growth and

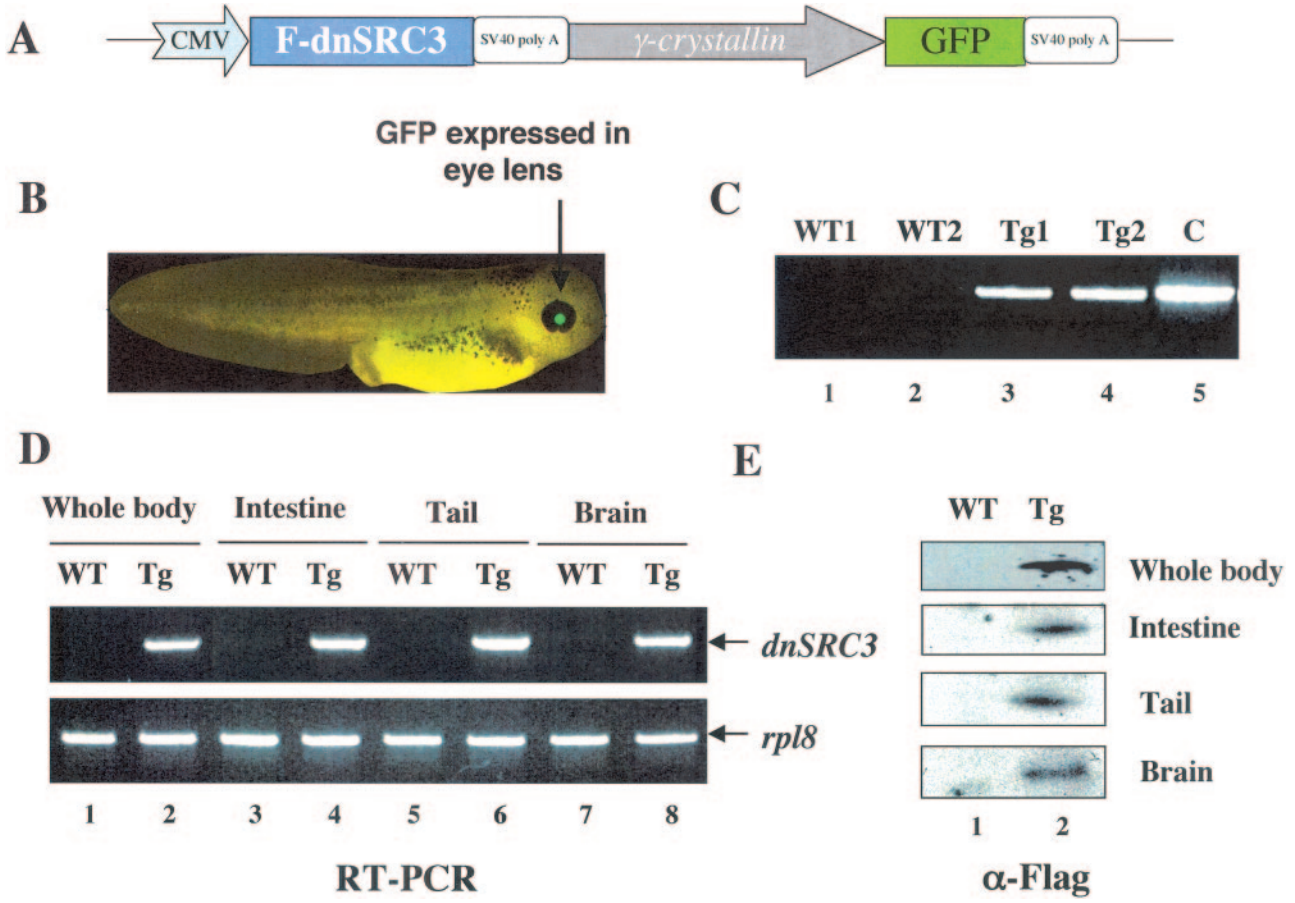

FIG. 4. Generation of transgenic animals expressing F-dnSRC3. (A) Schematic representation of the construct used for transgenesis. The constitutively active CMV promoter drives the expression of the transgene, F-dnSRC3, which is followed by the SV40 polyadenylation signal. The construct also harbors GFP under the *γ-crystallin* promoter as a marker to identify transgenic animals. (B) A transgenic *X. laevis* tadpole. The presence of GFP in the eye (green lens; arrow) indicates the presence of the transgene F-dnSRC3 in the tadpole. (C) The expression of the transgene correlates with the presence of green eyes. RNA isolated from two wild-type animals (WT1 and WT2) and two transgenic animals (Tg1 and Tg2, as identified by the presence of the GFP in the eyes) was subjected to RT-PCR using primers specific for the transgene. Lanes 1 and 2, wild-type animals; lanes 3 and 4, transgenic animals; lane 5, control PCR amplification by using the plasmid construct shown in panel A as the template. (D) RT-PCR shows that the transgene mRNA is expressed similarly in different tissues of dnSRC3 transgenic but not wild-type animals. Total RNA isolated from various tissues of wild-type (WT) and transgenic (Tg) tadpoles at stage 54 was analyzed by RT-PCR using the dnSRC3 transgene-specific primers. Lanes 1 and 2, whole body; lanes 3 and 4, intestine; lanes 5 and 6, tail; and lanes 7 and 8, brain. (E) Western blot analysis confirms the expression of F-dnSRC3 protein in different tissues of the transgenic animals. Lane 1, protein extract from a wild-type animal; lane 2, protein extract from a transgenic animal.

treatment conditions, because transgenic animals could be easily identified at the end of the treatment by their green eyes under a fluorescent microscope due to the GFP expression in the eyes (Fig. 4B). After the transgenesis, the wild-type and sibling transgenic (green-eyed) animals were reared together, and the transgenic animals developed apparently normally (at least after feeding begins at stage 45, when we started monitoring) up to the onset of metamorphosis compared to wild-type siblings. To verify the expression of F-dnSRC3 in the green-eyed transgenic animals, RNA from wild-type and sibling transgenic (green-eyed) tadpoles was isolated and subjected to RT-PCR, which revealed that green eyes correlated with the presence of the transgene mRNA in the tadpoles (Fig. 4C). Furthermore, analysis of the expression of the transgene in different tissues such as the intestine, tail, and brain showed similar expression levels in different organs (Fig. 4D). Western blot analysis confirmed similar levels of F-dnSRC3 protein in different organs of the transgenic but not wild-type animals (Fig. 4E).

To analyze the effect of the transgene on metamorphosis, we first subjected early-premetamorphic-stage animals (stage 45; 7 days old) to T3 treatment when wild-type animals first become competent to respond to T3. A 10 nM T3 treatment for 7 days led to the expected metamorphic changes in wild-type tadpoles (Fig. 5). The gills, which are the breathing organs in the tadpoles, regressed, reducing the size of the head (Fig. 5A, compare A2 and A5 to A1 and A4). The Meckel's cartilage of the lower jaw protruded, giving the head a triangular appearance (Fig. 5, compare A2 and A5 to A1 and A4) and the tail shortened (Fig. 5B). In contrast, little difference was observed between transgenic tadpoles treated with T3 (Fig. 5, A3 and A6, and 5B, Tg+T3) and the untreated wild-type tadpoles (Fig. 5, A1 and A4, and 5B, WT).

To study the effect on the transformation of other organs, we

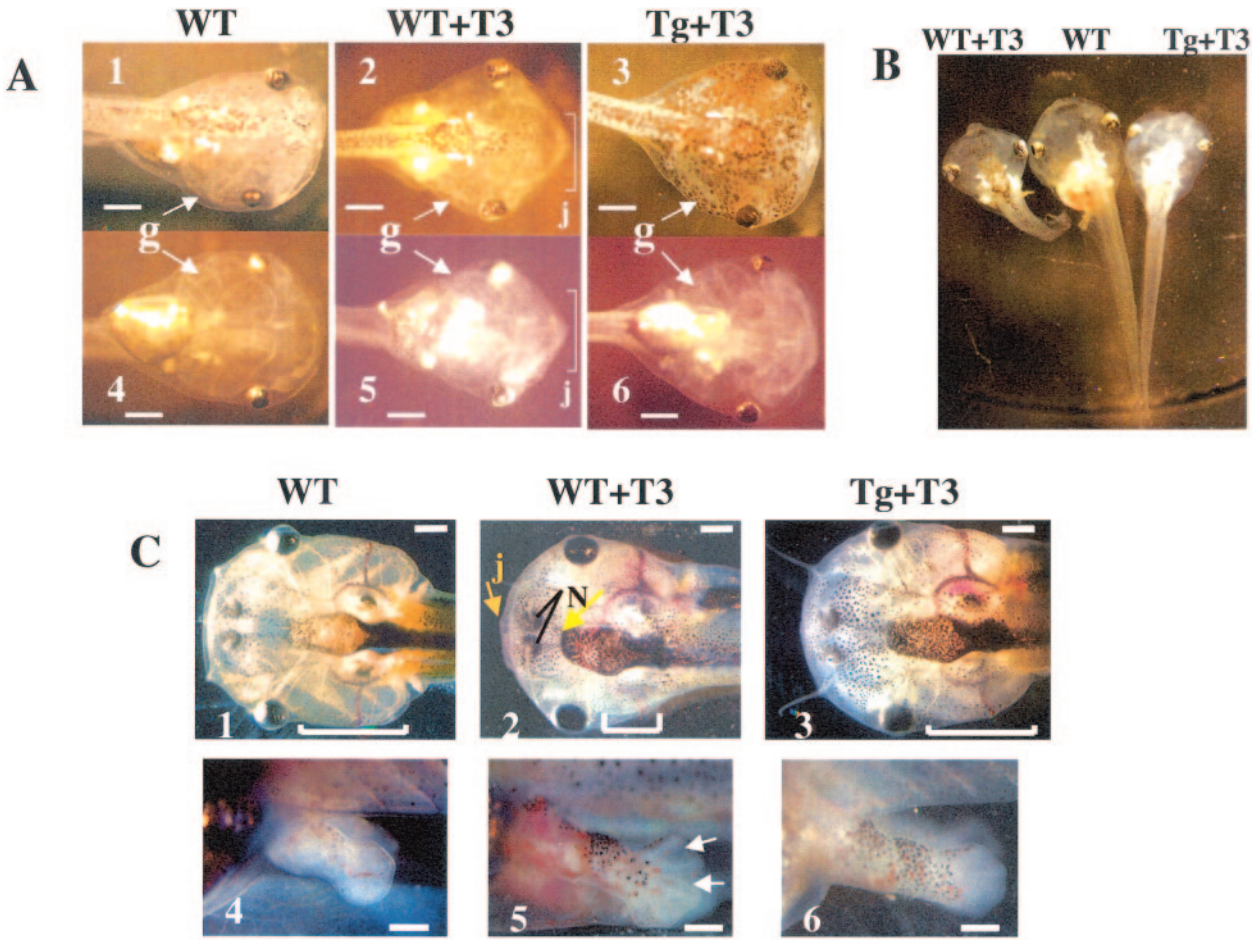

FIG. 5. Transgenic overexpression of dnSRC3 inhibits T3-induced metamorphosis. (A) Transgenic tadpoles overexpressing dnSRC3 fail to transform at the stage when wild-type tadpoles first become competent to respond to T3. One-week-old wild-type (WT) and transgenic (Tg) tadpoles (at about stage 45) were treated with 10 nM T3 for 7 days in 0.1× MMR. Panels 1 to 3, dorsal views of tadpoles; 4 to 6, corresponding ventral views of the tadpoles. Bar, 2 mm. Panels 1 to 4 show a wild-type tadpole without T3 treatment (WT). Panels 2 and 5 show a wild-type tadpole treated with 10 nM T3 (WT+T3). Note the regression of gills (g) and protrusion of the lower jaw (j) only in WT tadpoles treated with T3. Panels 3 and 6 show transgenic tadpoles overexpressing F-dnSRC3 treated with T3 (Tg+T3) exhibiting strong resistance to T3, as reflected by the absence of gill regression. (B) Wild-type (WT+T3) but not transgenic (Tg+T3) tadpoles overexpressing F-dnSRC3 had significant tail resorption upon T3 treatment. A wild-type animal (WT) without T3 treatment is shown as a control. (C) Overexpression of F-dnSRC3 inhibits T3-induced head and limb morphogenesis in late-premetamorphic-stage tadpoles. Wild-type and transgenic tadpoles at stage 54, right before limb morphogenesis, were treated with 5 nM T3 for 3 days. Transgenic tadpoles were identified by green fluorescence in the eye lens under a fluorescence microscope. As in the case of younger tadpoles shown in panels A and B, the characteristic T3-induced changes such as resorption of gills (bracketed) and development of the Meckel's cartilage leading to protrusion of the jaw (marked as j) were observed in the case of the wild-type tadpole treated with T3 (compare panel C2 to C1). In addition, the anterior end of the olfactory lobe (yellow arrow) is closer to the nostrils (marked as N) in wild-type animals treated with T3 (C2) in contrast to untreated wild-type animals (C1). These changes are not observed in dnSRC3 transgenic animals (C3). Furthermore, the development of the hind limbs is retarded in the transgenic animal (C6) compared to the wild-type animal treated with T3 (C5). The digits (white arrows) become obvious in the wild-type (C5) but not transgenic (C6) animals treated with T3. Bar, 2 mm (C1 to C3), 1 mm (C4 to C6).

analyzed tadpoles at stage 54, just prior to the onset of natural metamorphosis. At this stage, the hind limbs are about twice as long as their width with no differentiation into digits. After 3 days of 5 nM T3 treatment, limb morphogenesis (Fig. 5, C5), gill resorption and head remodeling (Fig. 5, C2) occurred in wild-type tadpoles. These treated tadpoles also had a shorter distance between the nostrils and the anterior end of the olfactory lobe compared to untreated ones (Fig. 5, C2 versus C1). The F-dnSRC3 transgenic tadpoles were impaired in all these transformations (Fig. 5, C3 and C6). Under our transgenic conditions, three out of four of the F_0 transgenic tadpoles in three independent experiments displayed such strong resistance to T3, while the remaining one in each independent experiment exhibited a partial resistance to the effects of T3 (not shown), presumably due to lower levels of transgene expression.

The effect of the F-dnSRC3 transgene on the metamorphosis of internal organs was studied by a histological analysis of the small intestine. The premetamorphic intestine is a simple tubular organ of a monolayer of epithelial cells with little connective tissue and muscles except in the single epithelial fold, the typhlosole, where connective tissue is abundant (57, 77). T3 treatment of premetamorphic tadpoles at stage 54 resulted in the typical metamorphic changes, including the

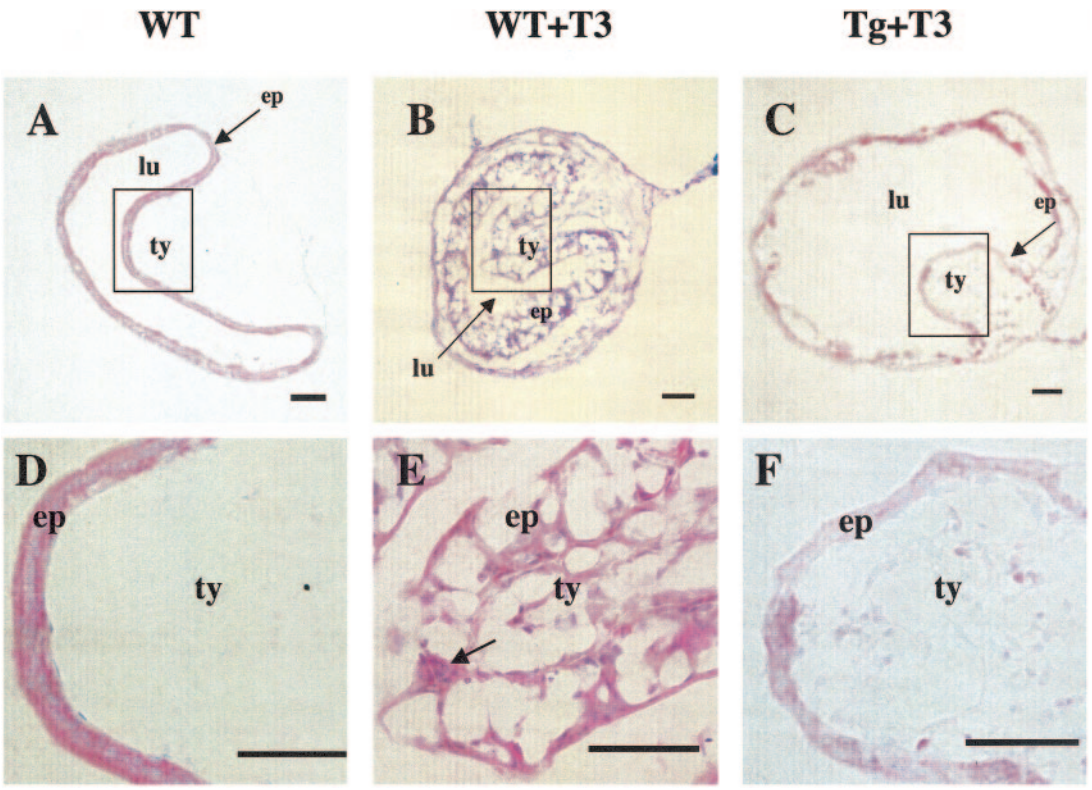

FIG. 6. Transgenic expression of F-dnSRC3 inhibits T3-mediated intestinal remodeling. Wild-type (WT) and transgenic (Tg) animals were treated with T3 as described for Fig. 5C, and the intestine was sectioned for analysis. (A to C) Cross sections of the small intestine of untreated wild-type (WT) tadpole and wild-type (WT+T3) and transgenic (Tg+T3) animals treated with T3, respectively. (D to F) A higher magnification of the intestinal sections shown in area delineated by boxes in panels A to C. The intestinal sections of wild-type animals (A) have a single fold, the typhlosole (ty), a single layer of aligned columnar epithelial cells (ep), and a thin connective tissue layer (except in the typhlosole) surrounding the epithelium. The intestinal sections of T3-treated wild-type tadpoles (B and E) exhibit degeneration of the larval epithelium, proliferation of adult epithelial cells (arrow), and thickening of the connective tissue layers. The transgenic animals treated with T3 (C and D) had few such changes. The lumen (lu) of these animals (C) remains large compared to that of wild-type animals treated with T3 (B). Bar, 50 μm.

degeneration of the larval epithelium, proliferation of adult epithelial cells, and increase in the thickness of the connective tissue (compare Fig. 6B to A and E to D). On the other hand, the intestine of F-dnSRC3 transgenic tadpoles treated with T3 resembled the intestine of an untreated or premetamorphic animal in structure, although intermediate transformation was evident (Fig. 6C and F). These results, together with observations from external morphological analysis, suggest that F-dnSRC3 inhibits T3-induced metamorphosis of most, if not all, organs and/or tissues.

Transgenic overexpression of F-dnSRC3 inhibits natural metamorphosis. We then examined the effects of the F-dnSRC3 transgene on natural metamorphosis by monitoring the natural development of transgenic tadpoles. While wild-type tadpoles complete metamorphosis within a little over 2 months (Fig. 7A), metamorphosis of the transgenic animals was delayed or inhibited. Some of the transgenic animals completed metamorphosis in 3 to 4 months while others died prior to the end of metamorphosis. A few tadpoles appeared to have completed their metamorphic program, except the resorption of the tail (Fig. 7B and C), in an extended period of 4 months. Massive tail resorption, i.e., noticeable change in tail lengths, naturally initiates around stage 62 when endogenous T3 and TR are at peak levels; the completion of tail resorption also marks the end of metamorphosis (12, 56), suggesting that tail resorption requires maximal levels of TR action. Thus, it is possible that it is easier to block tail resorption than other metamorphic changes. Our results would suggest that animals with high levels of F-dnSRC3 died due to inhibition of natural metamorphosis in many organs, although interference of F-dnSRC3 with other nuclear receptors cannot be ruled out completely. The animals with lower levels of transgene expression were able to complete metamorphosis in most organs but not in the ones requiring high levels of T3 induction, such as the tail. These different phenotypes observed were likely due to the relative levels of expression of the F-dnSRC3 transgene compared to the endogenous SRC3 and other coactivators. The increase in the expression of endogenous SRC3 during natural metamorphosis (47) might titrate out some of the effect of F-dnSRC3 during natural metamorphosis compared to T3 treatment of stage 54 tadpoles, where the endogenous SRC3 expression was low and the inhibition of T3-induced metamorphosis by F-dnSRC3 transgene was more dramatic (see above).

The F_1 generation of F-dnSRC3 transgenic animals also displays resistance to T3-induced metamorphosis. Some of the F_0 generation animals derived from the transgenic procedure were able to complete natural metamorphosis, although it was delayed compared to that of sibling wild-type animals. To elim-

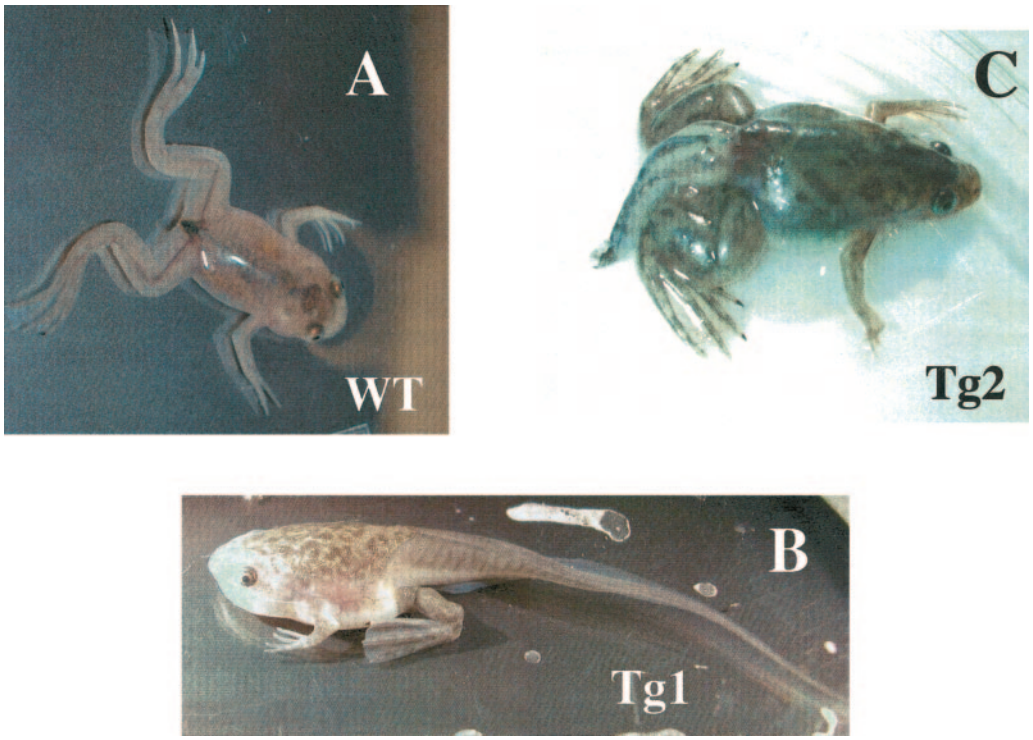

FIG. 7. Transgenic expression of F-dnSRC3 inhibits natural metamorphosis. Wild-type and transgenic tadpoles were allowed to undergo natural metamorphosis. (A) By the end of metamorphosis at stage 66, about 2 months postfertilization, the wild-type animals (WT) had no tail. (B and C) In contrast, two 4-month-old transgenic animals (Tg1 and Tg2) retained their tail but otherwise appeared to have undergone normal metamorphosis, e.g., their gills regressed and hind limbs developed. The animals eventually died, likely due to partial metamorphosis.

inate the unlikely possibility that the resistance to metamorphosis observed with the F_0 generation F-dnSRC3 transgenic animals were artifacts of transgenesis, we produced tadpoles of the F_1 generation by crossing a male transgenic frog with a female transgenic frog. The transgenic and wild-type offspring all developed normally; after reaching premetamorphic stage 54, the transgenic animals were treated with 5 nM T3 together with their wild-type siblings (as determined by observing eye color under a fluorescent microscope). Morphological examinations showed that similar to the F_0 animals, these transgenic animals exhibited a resistance to T3 (data not shown). The T3-treated transgenic tadpoles did not undergo gill resorption or head remodeling as seen with wild-type animals treated with T3 and remained essentially like the untreated wild-type animals (data not shown). In addition, RT-PCR analysis revealed that the gene induction pattern of T3-responsive genes was also impaired (data not shown). (It should be pointed out that different F_1 animals may have different levels of transgene expression depending upon whether they received transgene from the father or mother or both parents. However, under our experimental conditions, we failed to detect significant difference among the F_1 animals, suggesting all had sufficient F-dnSRC3 to inhibit T3-induced metamorphosis.) Thus, the T3-resistant phenotype was due to specific inhibition of the T3 signaling pathway by the F-dnSRC3 transgene.

The dominant negative SRC3 inhibits metamorphosis by blocking the activation of T3-responsive genes. To investigate the molecular mechanism by which F-dnSRC3 inhibits metamorphosis, we analyzed the expression of known T3 response genes in wild-type and transgenic animals treated with T3. We focused our studies on the intestine because it has been studied extensively at both morphological and molecular levels (56). We analyzed four early or direct T3-response genes, namely, *TRβA*, *TH/bZIP*, *stromelysin-3* (*ST3*), and *sonic hedgehog* (*xhh*) and a late or indirect T3 response gene, the bone morphogenic protein 4 gene *BMP4* (19, 30, 42, 46, 49, 60). All these genes are known to be upregulated in the intestine during T3 treatment or natural metamorphosis. As expected, all genes were induced in the intestine of premetamorphic wild-type tadpoles treated with T3 (Fig. 8, lanes 1 and 2). On the other hand, little induction was observed in transgenic tadpoles treated with T3 (Fig. 8, compare lanes 2 and 3). These results indicate that the F-dnSRC3 interfered with the activation of both early (direct) and late (indirect) T3 response genes, thereby blocking the entire metamorphic gene expression program and thus metamorphosis as well.

The F-dnSRC3 displaces the endogenous wild-type SRC3 from T3 target promoters without an effect on corepressor release in the transgenic animals. Based on the expression analyses and the functional studies in the frog oocyte, we hypothesized that the dominant negative SRC3 could compete out the recruitment of endogenous wild-type coactivators by liganded TR to target promoters. To test this possibility, we carried out ChIP assays on two T3-activated promoters, *TRβA* and *TH/bZIP*, in the intestine. We subjected wild-type and F-dnSRC3 transgenic premetamorphic tadpoles at stage 54 to T3 treatment and isolated the nuclei from the intestine for ChIP assays. T3 treatment of wild-type animals led to the recruitment

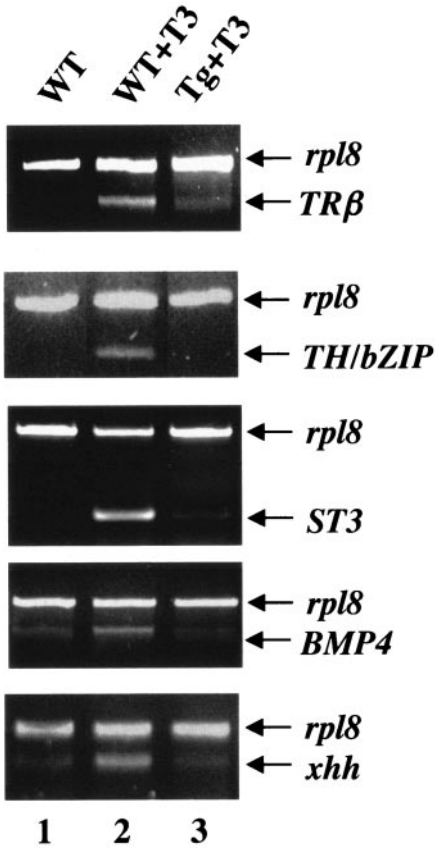

FIG. 8. Transgenic expression of F-dnSRC3 inhibits gene activation by T3. Wild-type (WT) and transgenic (Tg) tadpoles at stage 54 were treated with or without 5 nM T3 for 3 days. Total RNA was isolated from the intestine, and RT-PCR was performed to compare expression of known T3-regulated genes *TRβA*, *TH/bZIP*, *ST3*, *xhh*, and *BMP4*. The expression of the ribosomal protein L8 gene (*rpl8*) was used as an internal control.

of endogenous wild-type SRC3 and increased local acetylation of histone H4 at the promoters, accompanied by the release of corepressor SMRT (Fig. 9). In contrast, in the transgenic animals, T3 treatment led to the recruitment of F-dnSRC3 as shown by ChIP using an antibody against the Flag tag of the transgenic protein, and there was little increase in binding of endogenous SRC3 or acetylation level of histone H4 compared to the untreated wild-type animals (Fig. 9, compare Tg+T3 to WT). On the other hand, T3-induced release of the corepressor SMRT was expectedly not affected by the transgenic expression of F-dnSRC3. While the lack of availability of antibodies against other potential TR coactivators prevented the analysis of their recruitment, our results strongly suggest that F-dnSRC3 functions by preventing the binding of coactivator complexes essential for transcriptional activation of T3 target genes, thereby inhibiting the T3-induced metamorphic gene expression program and metamorphosis.

DISCUSSION

TRs are dual function transcription factors functioning as repressors in the absence of T3 and activators in the presence of T3 (38, 41, 66, 75). Unliganded TR interacts with corepressors, whereas ligand-bound TR recruits coactivators. Despite the in depth understanding of the properties and functions of the various cofactors in gene regulation by TRs, the developmental roles of these cofactors in nuclear receptor function in vivo largely remain to be explored. Gene knockout mice lacking coactivators sometimes have little or relatively mild phenotypes due to cofactor redundancy or embryonic lethal phenotypes, thus revealing little information about their roles in development. In addition, because these cofactors are often involved in multiple transcriptional regulatory pathways, it is difficult to pinpoint the role of a particular cofactor to a nuclear hormone receptor even when gene knockout and transgenesis result in easily identifiable phenotypes, such as mice deficient in p300, SRC1 to -3, or TRAP220 (21, 32, 33, 69, 72, 73). Here, we have made use of the total dependence of amphibian metamorphosis on T3 as a model to demonstrate for the first time that gene activation through coactivator recruitment, beyond derepression via release of corepressors, is required for TR-dependent developmental processes.

The ability of TR to repress and activate target genes in a T3-dependent manner and the expression of TR in tadpoles prior to the synthesis of endogenous T3 have led to a dual-function model for TR during frog development (52). The unliganded TR functions to repress T3-inducible genes to prevent precocious metamorphosis. When the animals grow to critical stages, endogenous T3 is synthesized, converting TR to an activator. This leads to the activation of the T3-inducible genes and thus tissue-specific metamorphosis. A role in gene repression by unliganded TR in premetamorphic tadpoles was supported by data showing the recruitment of the corepressors N-CoR, SMRT, and (more recently) TBLR1 to endogenous T3 response gene promoters in tadpoles and their release upon T3 treatment of the tadpoles (2, 53, 64). Additional evidence for gene repression involving HDAC complexes in premetamorphic tadpoles has come from the fact that inhibiting endogenous histone deacetylase activity with the drug trichostatin A leads to histone acetylation and activation of T3-responsive promoters (50, 51, 54). Thus, it is reasonable to believe that T3-induced release of corepressors when T3 becomes available is an important factor in the upregulation of T3-inducible genes required for metamorphosis. This requirement for release of repression by TR has been substantiated recently by the analyses of transgenic tadpoles overexpressing a dominant negative TR that can no longer bind T3. These animals exhibited arrested or delayed metamorphosis (2, 55), accompanied by the inhibition of T3-dependent gene regulation and the retention of corepressors at T3-regulated promoters (2), supporting the hypothesis that corepressor release is important for metamorphosis. However, these studies left unanswered whether activation above derepression is required for metamorphosis.

Here, we used a dominant negative form of *Xenopus* SRC3 (F-dnSRC3) overexpressed in transgenic animals to investigate the function of coactivators during metamorphosis. We showed that transgenic overexpression of F-dnSRC3 is sufficient to inhibit all aspects of T3-induced and natural metamorphosis that we analyzed. At the molecular level, F-dnSRC3 overexpression in transgenic tadpoles specifically blocked T3-induced activation of T3 response genes, e.g., *TRβA*, *TH/bZIP*, *ST3*, *xhh*, and *BMP4* in tadpoles. In addition, we showed that F-

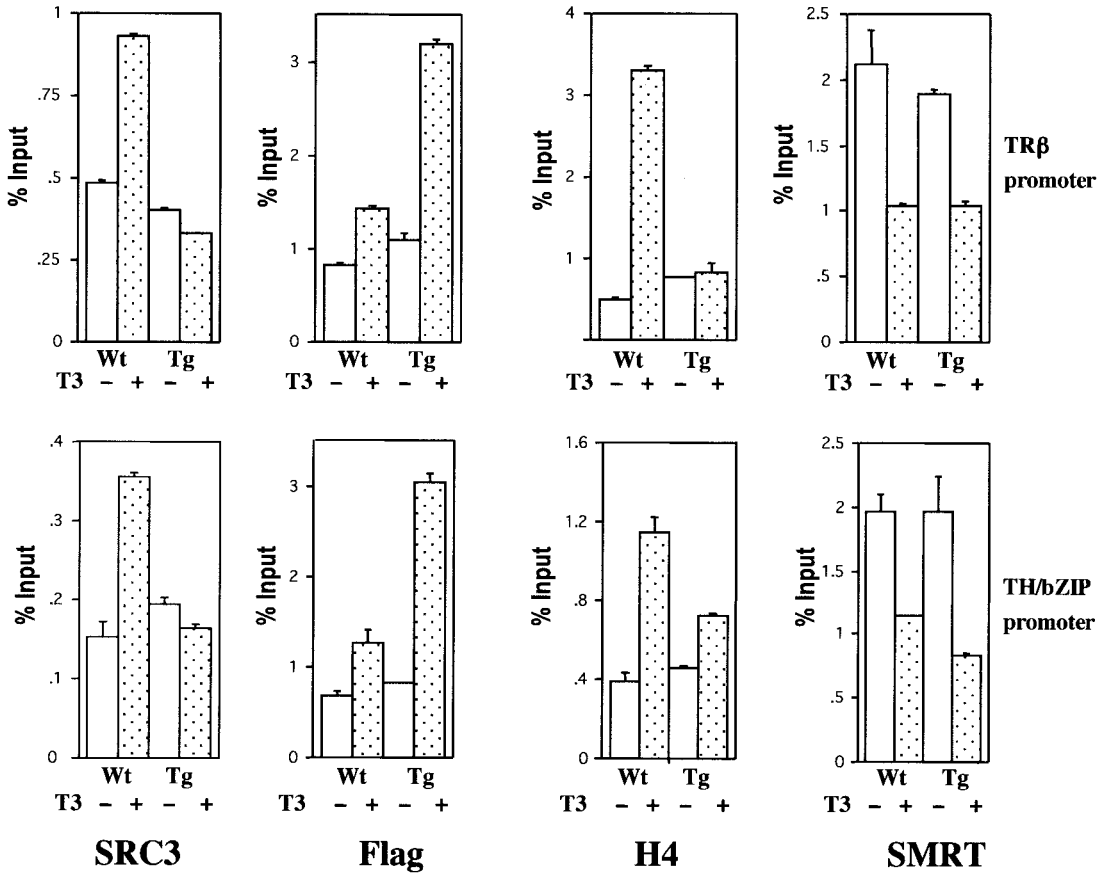

FIG. 9. Transgenic F-dnSRC3 competes with endogenous wild-type SRC3 for binding to liganded TR at T3-regulated promoters in the intestine, leading to reduced histone acetylation, but without an effect on T3-induced corepressor release. Wild-type (WT) and transgenic (Tg) animals at stage 54 were treated with 10 nM T3 for 2 days. Intestinal nuclei were isolated, and ChIP assays were performed using anti-TR, anti-SRC3 (for endogenous wild-type SRC3), antiacetylated histone H4, anti-SMRT (for endogenous corepressor SMRT), and anti-Flag (for F-dnSRC3 transgene) antibodies. The TRE regions of *TH/bZIP* and *TRβA* promoters were analyzed by real-time PCR after immunoprecipitation with the indicated antibodies. Note the reduced level or absence of endogenous SRC3 recruitment and the corresponding histone acetylation in T3-treated transgenic tadpoles compared to wild-type ones, while no difference in SMRT recruitment was observed.

dnSRC3 is recruited in a T3-dependent manner to target promoters and, more importantly, competes away the recruitment of endogenous SRC3 to these promoters, leading to reduced histone acetylation at the promoters. Expectedly, F-dnSRC3 did not interfere with the recruitment of endogenous corepressors such as SMRT by unliganded TR to the T3 target promoter or their release when T3 is present. Despite the corepressor release, T3-induced gene upregulation and tissue transformation were all inhibited in the transgenic animals, indicating that corepressor release plays only a minor role in gene regulation by T3 during frog development, contrary to the findings from transcription studies with tissue culture cells or frog oocytes.

Even though we have analyzed the recruitment of endogenous SRC3 but not other coactivators due to lack of reagents, F-dnSRC3 is likely to block the binding of other coactivators such as SRC1, SRC2, and p300 to TRs, as there is only a single ligand-induced coactivator-binding site on TRs. Thus, it is not surprising that F-dnSRC3 blocks metamorphosis in all tissues or organs examined, by blocking any potential tissue-specific or ubiquitous coactivator. Furthermore, the phenotypes and gene expression profiles of transgenic animals expressing F-dnSRC3 are essentially identical under our assay conditions to those of transgenic animals expressing a dominant negative TR (2, 55). These would suggest that F-dnSRC3 predominantly affects TR function during this developmental period. Such a conclusion may be understandable given the fact that TR is the central transcription factor for metamorphosis, both necessary and sufficient for mediating the effects of T3 during metamorphosis (2, 3). On the other hand, other nuclear hormone or orphan receptors are also likely to interact with F-dnSRC3. Their function will likely be inhibited by the transgenic F-dnSRC3 as well. However, the roles of these other receptors in metamorphosis are either unknown or secondary to TR action during metamorphosis, even in organs where some may participate, e.g., glucocorticoid receptor in the tail (no ligands for nuclear receptors other than T3 can induce morphological changes in premetamorphic tadpoles) (56). Therefore, the unique property of the metamorphosis model allowed us to correlate the developmental phenotypes to specific gene regulation pathways affected by F-dnSRC3, i.e., gene regulation by TR involving coactivators. More importantly, our results demonstrate that corepressor release is not sufficient for T3 to effect postembryonic organ remodeling and that coactivator recruitment is also required for the developmental effects of T3 in vivo.

In summary, while altering coactivator function through knockouts can lead to developmental defects in mice, the underlying molecular mechanisms are unknown, due to the involvement of the cofactors in transcriptional regulation by many diverse transcription factors and the difficulty in accessing and manipulating postembryonic development in mammals. Our use of F-dnSRC3, comprising only the nuclear receptor-interacting domain, restricts its effect to nuclear receptors. More importantly, the total dependence of the transformations of different organs and/or tissues on T3 makes TR the only transcription factor that controls initiation of the different changes in various organs during this metamorphic period. This unique situation allowed us to illustrate the first example where specific developmental defects are caused by alterations of specific gene regulation pathways involving nuclear receptors. Our experiments connected the phenotype of organ transformation inhibition with the blockade of TR-dependent gene expression pathways via a mutant dominant negative coactivator. In addition, while derepression appears to be a major component of gene activation by T3 in tissue culture cells or frog oocytes, it does not seem to be critical in developing animals, as demonstrated here, further underscoring the importance of in vivo experiments in understanding the molecular mechanisms of nuclear receptor function in development.

ACKNOWLEDGMENT

We thank other members of the group for helpful discussions.

REFERENCES

1. **Amano, T., K. Leu, K. Yoshizato, and Y.-B. Shi.** 2002. Thyroid hormone regulation of a transcriptional coactivator in *Xenopus laevis*: implication for a role in postembryonic tissue remodeling. Dev. Dyn. **223:**526–535.
2. **Buchholz, D. R., V. S.-C. Hsia, L. Fu, and Y.-B. Shi.** 2003. A dominant negative thyroid hormone receptor blocks amphibian metamorphosis by retaining corepressors at target genes. Mol. Cell. Biol. **23:**6750–6758.
3. **Buchholz, D. R., A. Tomita, L. Fu, B. D. Paul, and Y.-B. Shi.** 2004. Transgenic analysis reveals that thyroid hormone receptor is sufficient to mediate the thyroid hormone signal in frog metamorphosis. Mol. Cell. Biol. **24:** 9026–9037.
4. **Burrow, G. N., D. A. Fisher, and P. R. Larsen.** 1994. Maternal and fetal thyroid function. N. Engl. J. Med. **331:**1072–1078.
5. **Carswell, S., and J. C. Alwine.** 1989. Efficiency of utilization of the simian virus 40 late polyadenylation site: effects of upstream sequences. Mol. Cell. Biol. **9:**4248–4258.
6. **Chen, H., R. J. Lin, R. L. Schiltz, D. Chakravarti, A. Nash, L. Nagy, M. L. Privalsky, Y. Nakatani, and R. M. Evans.** 1997. Nuclear receptor coactivator ACTR is a novel histone acetyltransferase and forms a multimeric activation complex with P/CAF and CBP/p300. Cell **90:**569–580.
7. **Chen, J. D., and R. M. Evans.** 1995. A transcriptional co-repressor that interacts with nuclear hormone receptors. Nature **377:**454–457.
8. **Chubet, R. G., and B. L. Brizzard.** 1996. Vectors for expression and secretion of FLAG epitope-tagged proteins in mammalian cells. BioTechniques **20:** 136–141.
9. **Damjanovski, S., L. M. Sachs, and Y.-B. Shi.** 2002. Function of thyroid hormone receptors during amphibian development, p. 153–176. *In* A. Baniahmad (ed.), Methods in molecular biology: thyroid hormone receptors, vol. 202. Humana Press, Inc., Totowa, N.J.
10. **Davis, P. J., and F. B. Davis.** 1996. Nongenomic actions of thyroid hormone. Thyroid **6:**497–504.
11. **Ding, X. F., C. M. Anderson, H. Ma, H. Hong, R. M. Uht, P. J. Kushner, and M. R. Stallcup.** 1998. Nuclear receptor-binding sites of coactivators glucocorticoid receptor interacting protein 1 (GRIP1) and steroid receptor coactivator 1 (SRC-1): multiple motifs with different binding specificities. Mol. Endocrinol. **12:**302–313.
12. **Dodd, M. H. I., and J. M. Dodd.** 1976. The biology of metamorphosis, p. 467–599. *In* B. Lofts (ed.), Physiology of the amphibia. Academic Press, New York, N.Y.
13. **Feng, W., R. C. Ribeiro, R. L. Wagner, H. Nguyen, J. W. Apriletti, R. J. Fletterick, J. D. Baxter, P. J. Kushner, and B. L. West.** 1998. Hormone-dependent coactivator binding to a hydrophobic cleft on nuclear receptors. Science **280:**1747–1749.
14. **Feng, X., Y. Jiang, P. Meltzer, and P. M. Yen.** 2001. Transgenic targeting of a dominant negative corepressor to liver blocks basal repression by thyroid hormone receptor and increases cell proliferation. J. Biol. Chem. **276:**15066–15072.
15. **Flamant, F., and J. Samarut.** 2003. Thyroid hormone receptors: lessons from knockout and knock-in mutant mice. Trends Endocrinol. Metab. **14:**85–90.
16. **Forrest, D., E. Hanebuth, R. J. Smeyne, N. Everds, C. L. Stewart, J. M. Wehner, and T. Curran.** 1996. Recessive resistance to thyroid hormone in mice lacking thyroid hormone receptor beta: evidence for tissue-specific modulation of receptor function. EMBO J. **15:**3006–3015.
17. **Fraichard, A., O. Chassande, M. Plateroti, J. P. Roux, J. Trouillas, C. Dehay, C. Legrand, K. Gauthier, M. Kedinger, L. Malaval, B. Rousset, and J. Samarut.** 1997. The T3R alpha gene encoding a thyroid hormone receptor is essential for post-natal development and thyroid hormone production. EMBO J. **16:**4412–4420.
18. **Fu, L., D. Buchholz, and Y.-B. Shi.** 2002. A novel double promoter approach for identification of transgenic animals: a tool for in vivo analysis of gene function and development of gene-based therapies. Mol. Reprod. Dev. **62:** 470–476.
19. **Furlow, J. D., and D. D. Brown.** 1999. In vitro and in vivo analysis of the regulation of a transcription factor gene by thyroid hormone during Xenopus laevis metamorphosis. Mol. Endocrinol. **13:**2076–2089.
20. **Gauthier, K., O. Chassande, M. Plateroti, J. P. Roux, C. Legrand, B. Pain, B. Rousset, R. Weiss, J. Trouillas, and J. Samarut.** 1999. Different functions for the thyroid hormone receptors TRα and TRβ in the control of thyroid hromone production and post-natal development. EMBO J. **18:**623–631.
21. **Gehin, M., M. Mark, C. Dennefeld, A. Dierich, H. Gronemeyer, and P. Chambon.** 2002. The function of TIF2/GRIP1 in mouse reproduction is distinct from those of SRC-1 and p/CIP. Mol. Cell. Biol. **22:**5923–5927.
22. **Gothe, S., Z. Wang, L. Ng, J. M. Kindblom, A. C. Barros, C. Ohlsson, B. Vennstrom, and D. Forrest.** 1999. Mice devoid of all known thyroid hromone receptors are viable but exhibit disorders of the pituitary-thyroid axis, growth, and bone maturation. EMBO J. **13:**1329–1341.
23. **Guenther, M. G., W. S. Lane, W. Fischle, E. Verdin, M. A. Lazar, and R. Shiekhattar.** 2000. A core SMRT corepressor complex containing HDAC3 and TBL1, a WD40-repeat protein linked to deafness. Genes Dev. **14:** 1048–1057.
24. **Heery, D. M., E. Kalkhoven, S. Hoare, and M. G. Parker.** 1997. A signature motif in transcriptional co-activators mediates binding to nuclear receptors. Nature **387:**733–736.
25. **Hetzel, B. S.** 1989. The story of iodine deficiency: an international challenge in nutrition. Oxford University Press, Oxford, United Kingdom.
26. **Hong, H., K. Kohli, A. Trivedi, D. L. Johnson, and M. R. Stallcup.** 1996. GRIP1, a novel mouse protein that serves as a transcriptional coactivator in yeast for the hormone binding domains of steroid receptors. Proc. Natl. Acad. Sci. USA **93:**4948–4952.
27. **Horlein, A. J., A. M. Naar, T. Heinzel, J. Torchia, B. Gloss, R. Kurokawa, A. Ryan, Y. Kamei, M. Soderstrom, C. K. Glass, et al.** 1995. Ligand-independent repression by the thyroid hormone receptor mediated by a nuclear receptor co-repressor. Nature **377:**397–404.
28. **Ishizuka, T., and M. A. Lazar.** 2003. The N-CoR/histone deacetylase 3 complex is required for repression by thyroid hormone receptor. Mol. Cell. Biol. **23:**5122–5131.
29. **Ishizuya-Oka, A., Q. Li, T. Amano, S. Damjanovski, S. Ueda, and Y.-B. Shi.** 2000. Requirement for matrix metalloproteinase stromelysin-3 in cell migration and apoptosis during tissue remodeling in Xenopus laevis. J. Cell Biol. **150:**1177–1188.
30. **Ishizuya-Oka, A., S. Ueda, T. Amano, K. Shimizu, K. Suzuki, N. Ueno, and K. Yoshizato.** 2001. Thyroid-hormone-dependent and fibroblast-specific expression of BMP-4 correlates with adult epithelial development during amphibian intestinal remodeling. Cell Tissue Res. **303:**187–195.
31. **Ito, M., and R. G. Roeder.** 2001. The TRAP/SMCC/Mediator complex and thyroid hormone receptor function. Trends Endocrinol. Metab. **12:**127–134.
32. **Ito, M., C. X. Yuan, H. J. Okano, R. B. Darnell, and R. G. Roeder.** 2000. Involvement of the TRAP220 component of the TRAP/SMCC coactivator complex in embryonic development and thyroid hormone action. Mol. Cell **5:**683–693.
33. **Jepsen, K., O. Hermanson, T. M. Onami, A. S. Gleiberman, V. Lunyak, R. J. McEvilly, R. Kurokawa, V. Kumar, F. Liu, E. Seto, S. M. Hedrick, G. Mandel, C. K. Glass, D. W. Rose, and M. G. Rosenfeld.** 2000. Combinatorial roles of the nuclear receptor corepressor in transcription and development. Cell **102:**753–763.
34. **Jones, P. L., and Y.-B. Shi.** 2003. N-CoR-HDAC corepressor complexes: roles in transcriptional regulation by nuclear hormone receptors, p. 237–268. *In* J. L. Workman (ed.), Current topics in microbiology and immunology: protein complexes that modify chromatin, vol. 274. Springer-Verlag, Berlin, Germany.
35. **Kim, H. J., S. K. Lee, S. Y. Na, H. S. Choi, and J. W. Lee.** 1998. Molecular cloning of xSRC-3, a novel transcription coactivator from Xenopus, that is related to AIB1, p/CIP, and TIF2. Mol. Endocrinol. **12:**1038–1047.
36. **Kroll, K. L., and E. Amaya.** 1996. Transgenic Xenopus embryos from sperm

nuclear transplantations reveal FGF signaling requirements during gastrulation. Development **122:**3173–3183.
37. **LaFranchi, S.** 1999. Thyroid function in the preterm infant. Thyroid **9:**71–78.
38. **Lazar, M. A.** 1993. Thyroid hormone receptors: multiple forms, multiple possibilities. Endocr. Rev. **14:**184–193.
39. **Li, H., P. J. Gomes, and J. D. Chen.** 1997. RAC3, a steroid/nuclear receptor-associated coactivator that is related to SRC-1 and TIF2. Proc. Natl. Acad. Sci. USA **94:**8479–8484.
40. **Li, J., J. Wang, J. Wang, Z. Nawaz, J. M. Liu, J. Qin, and J. Wong.** 2000. Both corepressor proteins SMRT and N-CoR exist in large protein complexes containing HDAC3. EMBO J. **19:**4342–4350.
41. **Mangelsdorf, D. J., C. Thummel, M. Beato, P. Herrlich, G. Schutz, K. Umesono, B. Blumberg, P. Kastner, M. Mark, and P. Chambon.** 1995. The nuclear receptor superfamily: the second decade. Cell **83:**835–839.
42. **Metz, A., S. Knoechel, P. Buechler, M. Koester, and W. Knoechel.** 1998. Structural and functional analysis of the BMP-4 promoter in early embryos of Xenopus laevis. Mech. Dev. **74:**29–39.
43. **Nieuwkoop, P. D., and J. Faber.** 1956. Normal table of Xenopus laevis, 1st ed. North Holland Publishing, Amsterdam, The Netherlands.
44. **Nolte, R. T., G. B. Wisely, S. Westin, J. E. Cobb, M. H. Lambert, R. Kurokawa, M. G. Rosenfeld, T. M. Willson, C. K. Glass, and M. V. Milburn.** 1998. Ligand binding and co-activator assembly of the peroxisome proliferator-activated receptor-gamma. Nature **395:**137–143.
45. **Onate, S. A., S. Y. Tsai, M. J. Tsai, and B. W. O'Malley.** 1995. Sequence and characterization of a coactivator for the steroid hormone receptor superfamily. Science **270:**1354–1357.
46. **Patterton, D., W. P. Hayes, and Y. B. Shi.** 1995. Transcriptional activation of the matrix metalloproteinase gene stromelysin-3 coincides with thyroid hormone-induced cell death during frog metamorphosis. Dev. Biol. **167:**252–262.
47. **Paul, B. D., and Y.-B. Shi.** 2003. Distinct expression profiles of transcriptional coactivators for thyroid hormone receptors during Xenopus laevis metamorphosis. Cell Res. **13:**459–464.
48. **Rachez, C., and L. P. Freedman.** 2001. Mediator complexes and transcription. Curr. Opin. Cell Biol. **13:**274–280.
49. **Ranjan, M., J. Wong, and Y. B. Shi.** 1994. Transcriptional repression of Xenopus TR beta gene is mediated by a thyroid hormone response element located near the start site. J. Biol. Chem. **269:**24699–24705.
50. **Sachs, L. M., T. Amano, N. Rouse, and Y. B. Shi.** 2001. Involvement of histone deacetylase at two distinct steps in gene regulation during intestinal development in Xenopus laevis. Dev. Dyn. **222:**280–291.
51. **Sachs, L. M., T. Amano, and Y. B. Shi.** 2001. An essential role of histone deacetylases in postembryonic organ transformations in Xenopus laevis. Int. J. Mol. Med. **8:**595–601.
52. **Sachs, L. M., S. Damjanovski, P. L. Jones, Q. Li, T. Amano, S. Ueda, Y. B. Shi, and A. Ishizuya-Oka.** 2000. Dual functions of thyroid hormone receptors during Xenopus development. Comp. Biochem. Physiol. Biochem. Mol. Biol. **126:**199–211.
53. **Sachs, L. M., P. L. Jones, E. Havis, N. Rouse, B. A. Demeneix, and Y.-B. Shi.** 2002. N-CoR recruitment by unliganded thyroid hormone receptor in gene repression during *Xenopus laevis* development. Mol. Cell. Biol. **22:**8527–8538.
54. **Sachs, L. M., and Y.-B. Shi.** 2000. Targeted chromatin binding and histone acetylation in vivo by thyroid hormone receptor during amphibian development. Proc. Natl. Acad. Sci. USA **97:**13138–13143.
55. **Schreiber, A. M., B. Das, H. Huang, N. Marsh-Armstrong, and D. D. Brown.** 2001. Diverse developmental programs of Xenopus laevis metamorphosis are inhibited by a dominant negative thyroid hormone receptor. Proc. Natl. Acad. Sci. USA **98:**10739–10744.
56. **Shi, Y.-B.** 1999. Amphibian metamorphosis: from morphology to molecular biology. John Wiley & Sons, Inc., New York, N.Y.
57. **Shi, Y.-B., and A. Ishizuya-Oka.** 1996. Biphasic intestinal development in amphibians: embryogensis and remodeling during metamorphosis. Curr. Top. Dev. Biol. **32:**205–235.
58. **Shi, Y.-B., and V. C.-T. Liang.** 1994. Cloning and characterization of the ribosomal protein L8 gene from Xenopus laevis. Biochim. Biophys. Acta **1217:**227–228.
59. **Shiau, A. K., D. Barstad, P. M. Loria, L. Cheng, P. J. Kushner, D. A. Agard, and G. L. Greene.** 1998. The structural basis of estrogen receptor/coactivator recognition and the antagonism of this interaction by tamoxifen. Cell **95:**927–937.
60. **Stolow, M. A., and Y. B. Shi.** 1995. Xenopus sonic hedgehog as a potential morphogen during embryogenesis and thyroid hormone-dependent metamorphosis. Nucleic Acids Res. **23:**2555–2562.
61. **Takeshita, A., G. R. Cardona, N. Koibuchi, C. S. Suen, and W. W. Chin.** 1997. TRAM-1, a novel 160-kDa thyroid hormone receptor activator molecule, exhibits distinct properties from steroid receptor coactivator-1. J. Biol. Chem. **272:**27629–27634.
62. **Tata, J. R.** 1993. Gene expression during metamorphosis: an ideal model for post-embryonic development. Bioessays **15:**239–248.
63. **Tomita, A., D. R. Buchholz, K. Obata, and Y.-B. Shi.** 2003. Fusion protein of retinoic acid receptor a with promeyelocytic leukaemia protein or promyelocytic leukaemia zinc-finger protein recruits N-CoR-TBLR1 corepressor complex to repress transcription in vivo. J. Biol. Chem. **278:**30788–30795.
64. **Tomita, A., D. R. Buchholz, and Y.-B. Shi.** 2004. Recruitment of N-CoR/SMRT-TBLR1 corepressor complex by unliganded thyroid hormone receptor for gene repression during frog development. Mol. Cell. Biol. **24:**3337–3346.
65. **Torchia, J., D. W. Rose, J. Inostroza, Y. Kamei, S. Westin, C. K. Glass, and M. G. Rosenfeld.** 1997. The transcriptional co-activator p/CIP binds CBP and mediates nuclear-receptor function. Nature **387:**677–684.
66. **Tsai, M. J., and B. W. O'Malley.** 1994. Molecular mechanisms of action of steroid/thyroid receptor superfamily members. Annu. Rev. Biochem. **63:**451–486.
67. **Voegel, J. J., M. J. Heine, M. Tini, V. Vivat, P. Chambon, and H. Gronemeyer.** 1998. The coactivator TIF2 contains three nuclear receptor-binding motifs and mediates transactivation through CBP binding-dependent and -independent pathways. EMBO J. **17:**507–519.
68. **Voegel, J. J., M. J. Heine, C. Zechel, P. Chambon, and H. Gronemeyer.** 1996. TIF2, a 160 kDa transcriptional mediator for the ligand-dependent activation function AF-2 of nuclear receptors. EMBO J. **15:**3667–3675.
69. **Wang, Z., D. W. Rose, O. Hermanson, F. Liu, T. Herman, W. Wu, D. Szeto, A. Gleiberman, A. Krones, K. Pratt, R. Rosenfeld, and C. K. Glass.** 2000. Regulation of somatic growth by the p160 coactivator p/CIP. Proc. Natl. Acad. Sci. USA **97:**13549–13554.
70. **Wikstrom, L., C. Johansson, C. Salto, C. Barlow, A. C. Barros, F. Baas, D. Forrest, P. Thoren, and B. Veenstrom.** 1998. Abnormal heart rate and body temperature in mice lacking thyroid hormone receptor. EMBO J. **17:**455–461.
71. **Wong, J., and Y.-B. Shi.** 1995. Coordinated regulation of and transcriptional activation by Xenopus thyroid hormone and retinoid X receptors. J. Biol. Chem. **270:**18479–18483.
72. **Xu, J., L. Liao, G. Ning, H. Yoshida-Komiya, C. Deng, and B. W. O'Malley.** 2000. The steroid receptor coactivator SRC-3 (p/CIP/RAC3/AIB1/ACTR/TRAM-1) is requried for normal growth, puberty, female reproductive function, and mammary gland development. Proc. Natl. Acad. Sci. USA **97:**6379–6384.
73. **Yao, T. P., S. P. Oh, M. Fuchs, N. D. Zhou, L. E. Ch'ng, D. Newsome, R. T. Bronson, E. Li, D. M. Livingston, and R. Eckner.** 1998. Gene dosage-dependent embryonic development and proliferation defects in mice lacking the transcriptional integrator p300. Cell **93:**361–372.
74. **Yaoita, Y., Y. B. Shi, and D. D. Brown.** 1990. Xenopus laevis alpha and beta thyroid hormone receptors. Proc. Natl. Acad. Sci. USA **87:**7090–7094.
75. **Yen, P. M.** 2001. Physiological and molecular basis of thyroid hormone action. Physiol. Rev. **81:**1097–1142.
76. **Yoon, H.-G., D. W. Chan, Z. Q. Huang, J. Li, J. D. Fondell, J. Qin, and J. Wong.** 2003. Purification and functional characterization of the human N-CoR complex: the roles of HDAC3, TBL1 and TBLR1. EMBO J. **22:**1336–1346.
77. **Yoshizato, K.** 1989. Biochemistry and cell biology of amphibian metamorphosis with a special emphasis on the mechanism of removal of larval organs. Int. Rev. Cytol. **119:**97–149.
78. **Zhang, J., M. Kalkum, B. T. Chait, and R. G. Roeder.** 2002. The N-CoR-HDAC3 nuclear receptor corepressor complex inhibits the JNK pathway through the integral subunit GPS2. Mol. Cell **9:**611–623.
79. **Zhang, J., and M. A. Lazar.** 2000. The mechanism of action of thyroid hormones. Annu. Rev. Physiol. **62:**439–466.